# PARTITION OF IMPURITIES WITHIN TITANIA SLAG

**Krzysztof Borowiec**
Rio Tinto Iron & Titanium Inc., Canada

## ABSTRACT

*The content of gangue impurities in ilmenite and the $Ti^{4+}/Ti^{3+}$ ratio during smelting controls the distribution of impurities between pseudobrookite and glassy silicate. These two factors greatly affect the stability of these two phases in sulfate type slag.*

*The entire $SiO_2$ and CaO in the smelter feed solidify as constituents of the glassy silicate. For a $Ti^{4+}/Ti^{3+}$ ratio above 3.4, 95% of MgO in the melt enters the $M_3O_5$ phase and glassy silicate solidifies as a homogeneous phase which is easily devitrified during slag upgrading. Higher degrees of reduction trigger solidification of pyroxene within glassy silicate. In the pyroxene range, a 70-80% of MgO from the melt solidifies within the $M_3O_5$ phase. An excessive reduction leads to solidification of refractory glassy silicate saturated with forsterite. In the homogeneous range of glassy silicate, 62% of $Al_2O_3$ in the melt enters the $M_3O_5$ phase during slag solidification. In pyroxene and forsterite range, the fraction of $Al_2O_3$ solidified in $M_3O_5$ phase decreases to 50% and 40%, respectively. A high stability of glassy silicate for $Ti^{4+}/Ti^{3+}$ ratio lower than 2.6 prevents the required devitrification and also the transformation of original $M_3O_5$ phase into a three-phase combination composed of rutile, MgO-depleted pseudobrookite and MgO-enriched ilmenite during upgrading of Sorel slag to UGS product.*

*For different QMM slag grades, Th and U background levels in the pseudobrookite were found to be in the range of 10-20 ppm and 1-8 ppm, respectively. About 90% of radioactive isotopes in the smelter feed were entrapped within glassy silicate during slag solidification.*

*The smallest solidus-liquidus gap was measured for QMM slag containing the gangue impurities in the range of 1-2%. As expected, the highest expansion of solidus-liquidus gap occurred for Sorel slag containing 11-12% of gangue impurities. Sharp changes in the viscosity curves for Sorel and QMM slag corresponding to the final melting of slag are in agreement with liquidus temperature measurements.*

## INTRODUCTION

The $TiO_2$ pigment industry demands high quality feedstock for their processes. Ilmenite smelting to sulfate or chloride type $TiO_2$ - rich slag is an important part of ilmenite upgrading. The sulfate type slag is further upgraded by QIT to chlorinable feedstock by removing detrimental impurities by UGS process.

In carbothermic smelting of ilmenite pig iron is produced together with $TiO_2$ -rich slag. The mineralogy of the ilmenite and the ash content in carbon control the quality of tapped slag. The rock-type ilmenite being the solid solution of $FeTiO_3$-$MgTiO_3$-$Fe_2O_3$ associated with gangue silicates is smelted to sulfate type titania slag. The beach-sand ilmenite which consists of series of weathered ilmenite prior to the smelting is efficiently upgraded by rejecting gangue minerals. Such feed is smelted to chloride type titania slag. Both slags solidified as ferrous pseudobrookite, so-called $M_3O_5$ - phase, contain very small quantities of $TiO_2$, $TiO_{2-x}$, $Fe_o$ and glassy silicate rich in $SiO_2$.

The stoichiometric relationship between the composition of smelter feed and products of smelting is illustrated on Figure 1. The Ti-Fe-Mg-O tetrahedron was cut with four planes having the metal/oxygen ratio of 3/5, 2/3, 3/4 and 1. The location of the rock-type ilmenite is marked on the right side of the $M_2O_3$ - plane i.e., $FeTiO_3$-$MgTiO_3$-$Fe_2O_3$ diagram. The beach-type smelter feed is marked as a narrow strip on the $FeTiO_3$ - $TiO_2$ composition line.

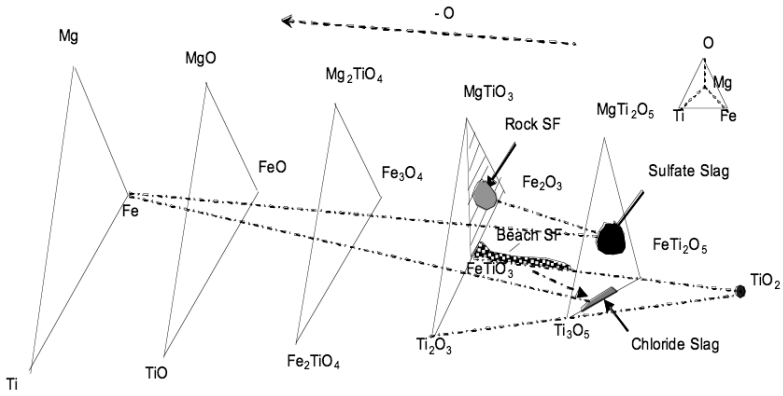


Figure 1: Stoichiometric relationship between ilmenite feed and smelting products

A difference in the location of commercial sulfate and chloride slag on the $M_3O_5$ - plane reflects the difference in impurity levels in their smelter feeds. The co-existence of pig iron with slag in the arc furnace is illustrated by thin dashed Fe-slag junctions.

The commercial slag could be further upgraded by reduction which enriches the pseudobrookite in the $Ti_3O_5$. Such enrichment results from the reduction of its FeO content and trapping additional quantities of MgO and $Al_2O_3$ in a glassy silicate phase during solidification of slag. In other words, the reduction pushes the pseudobrookite composition on the $M_3O_5$ plane towards its $Ti_3O_5$ corner. An excessive reduction leads to mushy slag with its composition approaching the $M_2O_3$ plane. The production and solidification aspects of $TiO_2$ - rich slag were discussed on the $TiO_2$ - $FeTiO_3$ - $Ti_2O_3$ diagram [1, 2, 3, 4]. The location of such diagram vs. $M_2O_3$ and $M_3O_5$ stoichiometric planes is also marked on Figure 1. The $TiO_2$ -$FeTiO_3$ - $Ti_2O_3$ ternary diagram exhibits a large primary field of $TiO_2$ and $Fe^o$ of the expense of ferrous pseudobrookite.

## Liqidus Isotherms of Pseudobrookite

In general, during solidification of $TiO_2$-rich slag the impurities are partitioned between ferrous pseudobrookite and the $SiO_2$-rich glassy phase. The compositions of solidified pseudobrookite of TTI slag (pilot tests), commercial Sorel (QIT) and RBM slag and different QMM slag (pilot tests) are marked on $FeTi_2O_5$-$MgTi_2O_5$-$Ti_3O_5$ diagram presented on Figure 2. The compositions of $M_3O_5$- phase solidified from these slags were determined by microprobe or EDX techniques. In the case of QMM slag, the composition of $MgTi_2O_5$ on the diagram represents the solid solution of $(Mg,Mn)Ti_2O_5$ - $Al_2TiO_5$. The liquidus isotherms generated by FACT separated by 10°C are marked as thin lines on the diagram. The dashed line at $Ti^{4+}/Ti^{3+}$ = 2.65 marks the degree of reduction of RBM slag determined for a bulk sample.

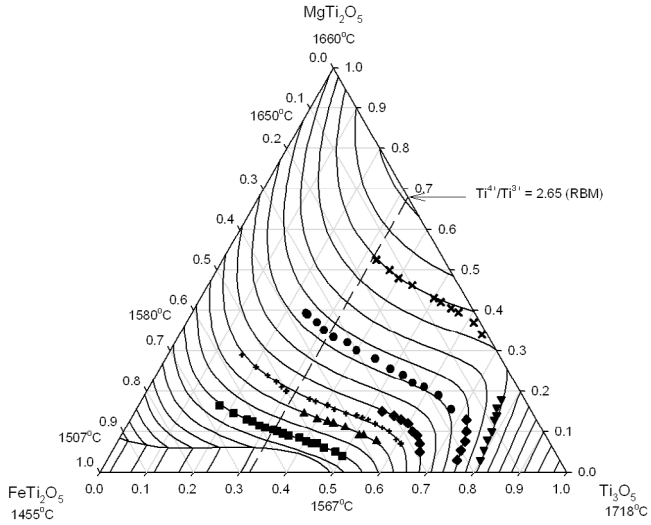


Figure 2: Liquidus isotherms in $FeTi_2O_5$-$MgTi_2O_5$-$Ti_3O_5$ system

According to Eriksson *et al*. [5]. $Ti_3O_5$ and $MgTi_2O_5$ melt congruently at 1718°C and 1660°C, respectively, while $FeTi_2O_5$ melts peritectically at 1455°C. Grau [6] reported melting of $FeTi_2O_5$ at 1480°C. As seen, FACT shows eutecticum in the vicinity of $FeTi_2O_5$ which is heading towards a composition of $(FeTi_2O_5)0.5(Ti_3O_5)0.5$.

According to the FACT calculation, a higher content of $MgTi_2O_5$ and $Ti_3O_5$ in the melt leads to a higher liquidus temperature of pseudobrookite. As seen, the composition of solidified pseudobrookite is varied in a wide range of degrees of reduction. For example, for Sorel and RBM slag, the $Ti^{4+}/Ti^{3+}$ ratio of $M_3O_5$ phase was varied from 1.2 to 4.5. In the similar reduction range, the pseudobrookite was solidified from 80% $TiO_2$ QMM slag.

The increase in degree of reduction during smelting of QMM ilmenite narrowed the $Ti^{4+}/Ti^{3+}$ range in which the pseudobrookite solidified. For example, the pseudobrookite of 95%$TiO_2$ QMM slag located on two liquidus isotherms was solidified in the $Ti^{4+}/Ti^{3+}$ range of 0.8-1.3. The entire pseudobrookite of 97% $TiO_2$ QMM slag solidified as $(Ti_3O_5)0.75$ $(MeTi_2O_5)0.25$ in the $Ti^{4+}/Ti^{3+}$ range of 0.75-0.8.

As seen, the composition of solidified pseudobrookite from different slags strictly follows the liquidus isotherms predicted by FACT. It indicates a narrow solidus-liquidus gap of pseudobrookite of sulfate and chloride type slags. A narrow gap is expected for QMM slag containing 2% of gangue impurities, however, 11-12% of gangue impurities in Sorel slag are expected to broaden the solidus-liquidus gap of its pseudobrookite.

## Glassy Silicate Phase of Sulfate Slag

The immiscibility gap in the $TiO_2/Ti_2O_3$-$SiO_2$ system drives the partition of gangue impurities between the $M_3O_5$ phase and the glassy silicate phase during solidification. Figure 3 presents the partition of gangue impurities in a wide range of $Ti^{4+}/Ti^{3+}$ ratios of solidified pseudobrookite of TTI and Sorel slag.

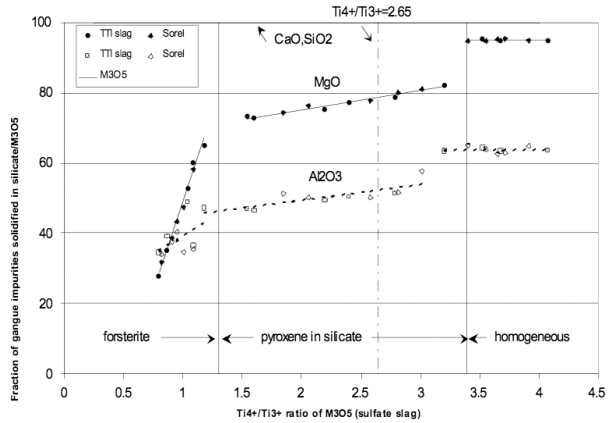


Figure 3: Partition of gangue impurities between $M_3O_5$ and glassy silicate phase

As seen, the entire $SiO_2$ and CaO in the smelter feed are solidifying as constituents of the glassy silicate. The $SiO_2$ and CaO background in the $M_3O_5$ - phase of commercial slag is well below 0.1% and it only increases slightly for a higher ratio of $Ti^{4+}/Ti^{3+}$. FeO content in the glassy silicate controls its degree of devitrification during upgrading of Sorel slag by UGS process [7]. For $Ti^{4+}/Ti^{3+}$ ratio above 3.4, the glassy silicate solidified as a homogeneous phase containing 5-7% of FeO. In the homogeneous range, 95% of MgO in the melt enters the $M_3O_5$ phase during solidification.

Higher degrees of reduction drive the solidification of pyroxene-$(Mg,Ca,Fe)SiO_3$ within glassy silicate containing 2-3% of FeO. In the pyroxene range, 70-80% of MgO in the melt solidified within the $M_3O_5$ phase. Glassy silicate saturated with pyroxene exhibits a higher stability which leads to a less efficient devitrification during upgrading of slag via UGS process. In other words, the fraction of glassy silicate which remains in its original unleachable form after processing of slag via UGS process depends on the $Ti^{4+}/Ti^{3+}$ ratio. The lowest $Ti^{4+}/Ti^{3+}$ ratio for Sorel slag that still permits the achievement of sufficient devitrification of glassy silicate was found to be 2.6. An excessive reduction leads to the solidification of glassy silicate saturated with forsterite - $(Mg,Fe)_2SiO_4$. In the forsterite range, 30-65% of MgO in the melt solidifies within the pseudobrookite lattice. It leads to refractory glassy silicate resulting in poor devitrification during upgrading of slag via UGS process.

The partition of $Al_2O_3$ between glassy silicate and $M_3O_5$ phase is represented by dashed line on Figure 3. As seen, there is a similar trend in partition of $Al_2O_3$ between the glassy silicate and the $M_3O_5$ phase as that for MgO, but the effect of $Ti^{4+}/Ti^{3+}$ ratio is less pronounced. In the homogeneous range of glassy silicate, 62% of $Al_2O_3$ in the melt enters $M_3O_5$ phase during solidification. In the pyroxene and forsterite range, the fraction of $Al_2O_3$ solidified in $M_3O_5$ phase decreases to 50% and 40%, respectively. The partition results presented above were obtained for the $SiO_2$ / MgO and $SiO_2$/ $Al_2O_3$ ratio of the commercial smelter feed for Sorel and TTI slag.

## Glassy Silicate Phase of Chloride Slag

A lower content of gangue impurities in the smelter feed for chloride slag leads to a smaller volume of glassy silicate. The example of a typical glassy silicate phase of 97%$TiO_2$ QMM slag is presented on Figure 4.

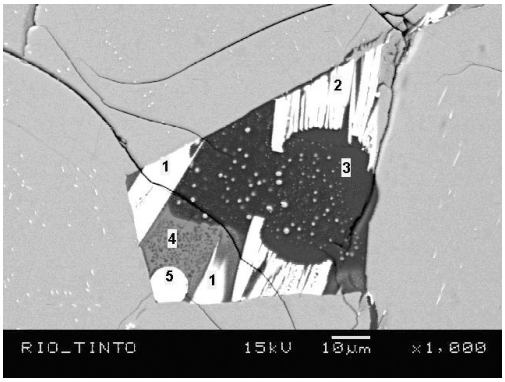


Figure 4: Back-scattered EDX picture of QMM slag

The radioactivity associated with the weathered ilmenite concentrate ends-up almost entirely in the $TiO_2$-rich melt. A high affinity of radioactive isotopes to $SiO_2$ and CaO drives a highly preferential solidification of Th and U isotopes in the glassy silicate. The entrapment of radioactive oxides within the glassy silicate is illustrated on Figure 4. The freezing front of pseudobrookite squeezed out the $SiO_2$-rich melt which solidified as the following multiphase assemblage: 1-radioactive phase: $TiO_2$-50.9%, $SiO_2$-17.2%, CaO-7.1%, $Ce_2O_3$-10.3%, $Nd_2O_3$-3.9%, $ThO_2$-8.1%, $UO_3$-0.8%; 2-radioactive phase: $TiO_2$-52.3%, $SiO_2$-18.2%, CaO-7.2%, $Ce_2O_3$-9.6%, $Nd_2O_3$-3.2%, $ThO_2$-8.2%, $UO_3$-0.5%; 3 - glassy silicate saturated with $TiO_2$; $SiO_2$- 83.9%, $TiO_2$-5.5%, $Al_2O_3$-5.1%, CaO-3.4%, $K_2O$-1%; 4-glassy silicate saturated in $SiO_2$: $SiO_2$-64.5%, CaO-13.8%, $TiO_2$- 8.4%, $Al_2O_3$ -6.9%, MnO-4.1%, FeO-1.4%; 5-metallic iron droplet.

The bright spots within the $M_3O_5$ phase represent tiny micro-droplets of $Fe^o$ and $TiO_2$ resulting from the following redox reaction $(2Ti^{3+}) + (Fe^{2+}) = 2Ti^{4+}_{(s)} + Fe^o$. The number of precipitated iron and $TiO_2$ micro-droplets increases with an increase of $Ti^{3+}$ content in the melt.

The shape of $^{232}Th^+$ and $^{238}U^+$ ion depth profile recorded by the SEMS technique from the pseudobrookite phase of QMM slag showed the uniform distribution of Th and U across the $M_3O_5$ phase. For different QMM slag grades, the Th and U background level in pseudobrookite was found to be in the range of 10-20 ppm and 1-6 ppm, respectively. The SIMS results indicate that 90% of radioactive isotopes in the smelter feed were entrapped within the glassy silicate during slag solidification. In other words, the glassy silicate in the chloride type slag acts as a trap for radioactive impurities.

## Solubility of $Tho_2$ in Pseudobrookite Phase

According to Lambert *et al*. [8], $ThTi_2O_6$ was found to exist in a wide range of oxygen potentials coexisting with Ti-oxides from $TiO_2$ up to $Ti_3O_5$. The solid solubility limits of $ThO_2$ in $Ti_4O_7$ and $Ti_3O_5$ as obtained from the solidified melt by the SIMS technique are found to be 700 and 600 ppm, respectively.

The same technique was used to determine the solubility of $ThO_2$ in pseudobrookite of QMM slag free of glassy silicate inclusions. The different mixtures of $TiO_2$, $Fe_2O_3$, $Fe^o$

and $ThO_2$ were heated in a Mo-crucible in a *graphite furnace* in argon. The resulting melts were solidified to $M_3O_5$ phase and small quantities of $TiO_{2-x}$ and Feo inclusions. The microprobe and SIMS techniques were used to determine the $Ti^{4+}/Ti^{3+}$ ratio and Th background in the $M_3O_5$ phase.

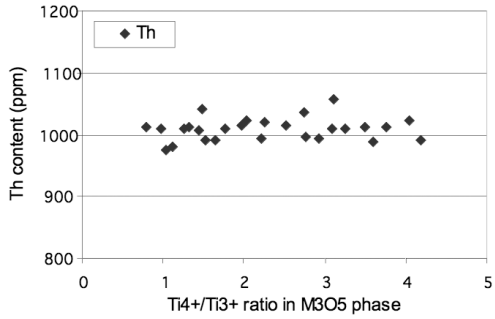


Figure 5: Th content in $M_3O_5$ phase saturated with $ThTi_2O_6$

The entry of $Th^{4+}$ into the $M_3O_5$ lattice is governed by several factors such as the ionic radii and ionic charge of ions involved. The ionic radii of $Th^{4+}$, $Ti^{4+}$ and $Ti^{3+}$ are $0.11\times10^{-9}$, $0.07\times10^{-9}$ m and $0.08\times10^{-9}$ m, respectively. If the difference in ionic radii is greater than 15% of the smaller ion, partial substitution may occur, provided that the size difference does not affect the coordination number. In the case of $Th^{4+}$ and $Ti^{4+}$ this difference is 57%, which indicates very limited substitution.

Figure 5 presents the effect of degree of reduction on Th content in the $M_3O_5$ phase. As seen, the contamination of $M_3O_5$ with Th was found at the 1000 ppm level in a wide range of $Ti^{4+}/Ti^{3+}$ ratios. The excess of $ThO_2$ used in the preparation of starting mixture for melting was solidified as tiny spots of $ThTi_2O_6$.

A steady accumulation of glassy silicate loaded with radioactive impurities in the cyclones of commercial chlorinators prevents the transfer of radioactivity to $TiO_2$ pigment. In addition, the entrapment of 90% of radioactive elements in the glassy silicate suggests that the chlorite type slag could be decontaminated prior to the chlorination by selective leaching of the glassy silicate. In other words, the transfer of radioactivity from slag to pigment during chlorination is controlled by the contamination level of smelter feed with $SiO_2$ and CaO. For a given radioactivity level, lower content of $SiO_2$ and CaO in the smelter feed leads to elevated level of radioactivity in the $M_3O_5$ phase which results in a higher contamination of pigment with radioactive impurities.

## Melting Point Determination

Small pieces of slag, about 3-4 mm cross-section, were heated in a *graphite furnace* in argon and the fusion of slag was observed optically. The sample temperature in the furnace was measured with calibrated optical pyrometer. The temperatures in the parallel tests were also measured with a Pt6Rh-Pt30Rh thermocouple placed within a Mo protection tube. The preliminary tests were performed with the slag pieces resting on vitreous carbon or rutile substrate. As soon as a liquid phase appeared it reacted strongly with the substrate, regardless of whether it was vitreous carbon or rutile. Microprobe analysis of the sample after melting the slag on vitreous carbon showed that practically all FeO has been reduced to metal, a part of $M_3O_5$ was reduced to Ti(OC) and the remaining part was reduced to practically pure $Ti_3O_5$ and $Ti_2O_3$ with a melting point of 1720-1740ºC for all slags.

The melting point tests for Sorel slag on $TiO_2$ substrate gave initial melting at 1610°C and complete melting at 1720°C. The solidified slag was examined by microprobe and XRD techniques, which showed the occurrence of $M_3O_5$ with unexpectedly high content of $TiO_2$ and $TiO_{2-x}$. Quick dissolution of a part of $TiO_2$ substrate in the melt produced the sample slag saturated with $TiO_2$.

The initial melting for Sorel slag on Mo substrate occurred at about 1578°C, and the complete melting at 1712°C. SEM investigation of the slag after experiment showed that all of the original $Fe^o$ micro-droplets in the slag sink had then diffused into Mo substrate forming a solid solution. Microprobe analysis carried out prior and after melting showed that the FeO content of slag had been affected negligibly by melting. The same measurements for RBM slag carried out on Mo substrate gave initial melting at 1582°C and complete melting at 1662°C. For 90%$TiO_2$ QMM slag solidus and liquidus were measured at 1558°C and 1620°C, respectively.

The solidus and liquidus temperature for the $FeTi_2O_5$-$Ti_3O_5$ system predicted by FACT is presented on Figure 6. Also, the initial and final melting temperatures for Sorel, RBM and 90%$TiO_2$ QMM slag measured on Mo substrate were marked. As expected, the highest expansion of solidus-liquidus gap occurred for Sorel slag containing 11-12% of gangue impurities. As seen, the gangue impurities tend to increase the final melting temperature of pseudobrookite having a small effect on the freezing temperature of slag.

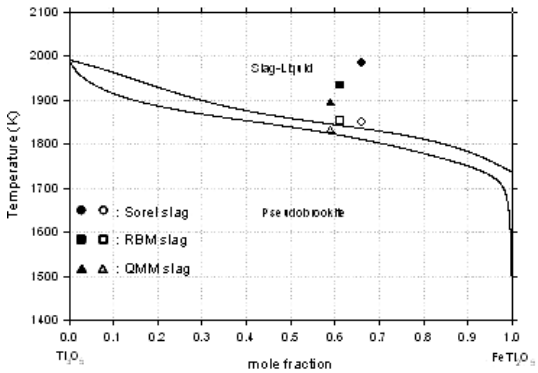


Figure 6: $FeTi_2O_5$-$Ti_3O_5$ system with melting point measurements

The final freezing point of 90% $TiO_2$ QMM is located on the solidus of $FeTi_2O_5$-$Ti_3O_5$ system predicted by FACT. As seen, for a similar bulk ratio of $Ti^{4+}/Ti^{3+}$ the solidus-liquidus gap gradually expands as gangue impurities in the melt are increased. This means that the gangue impurities tend to stabilize liquid $M_3O_5$ phase and also extend its range of stability to lower oxygen potentials.

## Viscosity of High $Tio_2$ Slag and Ilmenite

Tuset [9] found that the viscosity of completely molten samples from $TiO_2$-$Ti_2O_3$-$MgTiO_3$ system ranged from 50 to 100 cps and was independent of the slag composition and changes in slag temperature. Handfield *et al.* [10] have shown that when Sorel slag samples are completely molten, viscosity was as low as 30 cps. Furthermore, the viscosity value is independent of temperature, and the variation of FeO from 3.3 to 15 wt% did not seem to influence the viscosity of the Sorel slag. A step change in the viscosity observed on cooling corresponds to initial crystallization of pseudobrookite.

A step change in the viscosity curve of Sorel slag at 1709°C corresponds to the final melting of sample. This temperature is in close agreement with the liquidus temperature of 1712°C measured in this work. The same viscosity measurement technique was used for 95% $TiO_2$ QMM slag and ilmenite smelter feed for Sorel slag.

Figure 7 compares the viscosity of these melts with Handfield's viscosity values for Sorel slag. As seen, the step change in the viscosity values of 95% $TiO_2$ QMM slag occurred at 1613°C indicating the onset of crystallization of $M_3O_5$ phase from the melt. It should be noted that the liquidus temperature for 90%$TiO_2$ QMM slag was found to be 1620°C.

Ilmenite melts at 1377°C and its viscosity data was recorded in the temperature range of 1400 - 1680°C. At 1400°C the melt exhibits viscosity of 123 cps which gradually decreases reaching 40 cps at 1670°C. It should be noted that at the smelting temperature the molten slag and molten feed exhibit practically the same viscosity.

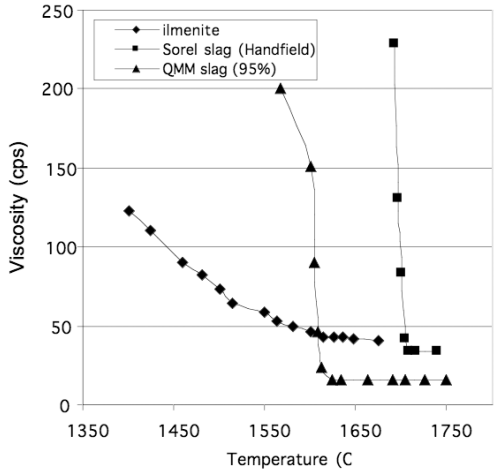


Figure 7: Viscosity of ilmenite and QMM slag

A very low viscosity seems to be a characteristic property for pure FeO, MgO, MnO, CaO and $Al_2O_3$. All of these oxides have viscosity of the order of 50cps near their melting points. It was observed that the addition of semiconducting $TiO_2$ or $Ti_2O_3$ to these oxides visibly decreased the viscosity and increased the electronic conductivity.

The viscosity of melt containing $Ti_2O_3$- 95%, FeO-2%, $SiO_2$-1%, MgO-0.5% and MnO-0.5% at 1750°C was measured to be 19.7cps i.e., slightly above viscosity for 95% $TiO_2$ QMM slag. The viscosity of $TiO_2$- slag is not visibly affected by $Ti^{3+}$ and gangue impurities content in the melt.

## CONCLUSIONS

The impurities from the smelter feed and coal have negligible effect on the viscosity, tapping behavior and solidus temperature of $TiO_2$-rich slag. However, the gangue impurities of the $TiO_2$-rich melt control the stability of the pseudobrookite and glassy silicate. The impurities level and $Ti^{4+}/Ti^{3+}$ ratio determine the degree of transformation of pseudobrookite to the combination of rutile, MgO-depleted pseudobrookite and MgO-enriched ilmenite during the processing of Sorel slag via the UGS process. The $Ti^{4+}/Ti^{3+}$ ratios lower than 2.6 lead to a poor transformation of original $M_3O_5$ phase into above-mentioned three -phase combination and also to insufficient devitrification of glassy silicate.

It results in unacceptable levels of MgO and CaO in the UGS product. The glassy silicate in the chloride type slag acts as a trap for radioactive impurities. For different QMM slag grades, the Th and U background levels in pseudobrookite were found to be in the range of 10-20 ppm and 1-6 ppm, respectively. 90% of radioactive isotopes in the smelter feed were entrapped within the glassy silicate. The chloride type slag could be decontaminated prior to the chlorination by caustic leaching of glassy silicate.

## REFERENCES

**Pistorius, P. C.** (2007). *Ilmenite Smelting: the Basics*. The 6th International Heavy Minerals Conference 'Back to Basics', The Southern African Institute of Mining & Metallurgy, 2007, pp. 75-84. [1]

**Pistorius, P. C. & Coetzee, C.** (2003). *Physicochemical Aspects of Titanium Slag Production & Solidification*. Metallurgical & Materials Transaction B. Vol. 34B, pp. 581-588. [2]

**Rosenqvist, T**. (1992). *Ilmenite Smelting*. Transactions of the Technical University of Kosice. Vol. 2, special issue, pp. 40-46. [3]

**Elstad, H., Eriksen, J. M., Hildal, A., Rosenqvist, T. & Seim. S.** (2007). *Equilibrium between Titania Slags and Metallic Iron*. The 6th International Heavy Minerals Conference 'Back to Basics', The Southern African Institute of Mining and Metallurgy, 2007, pp. 35-42. [4]

**Eriksson, G., Pelton, A. D. & Woermann, E.** (1996). *Measurement & Thermodynamic Evaluation of Phase Equilibria in the Fe-Ti-O System*. Ber. Bunsenges. Phys. Chem., Vol. 100, pp. 1839-1849. [5]

**Grau, A. E. & Poggi, D.** (1978). *Physico-Chemical Properties of Molten Titania Slag*. Annual Volume 1978, Metallurgical Society of Canada, Institute of Mining & Metallurgy, Montreal, pp. 97-102. [6]

**Borowiec, K., Grau, A. E., Guegin, M. & Turgeon, J. F.** (1998). *Method to Upgrade Titania Slag and Resulting Product*. US Patent 5,830,420. [7]

**Lambert, N. & Borowiec, K.** (2000). Standard Gibbs Free Energy of Formation of $ThTi_2O_6$ from Oxides. *Journal of Alloys and Compounds*, Vol. 297, pp. 266-269. [8]

**Tuset, J. Kr.** (1968). *Viscosity of $TiO_2$-rich Melts*. Kr. Tidsskr. Kjemi, Bergv., Metallurgi, Vol. 28, pp. 232-238. [9]

**Handfield, G. & Charette, G. G.** (1971). *Viscosity and Structure of Industrial High $TiO_2$ Slags*. Canadian Metallurgical Quarterly, Vol. 10(3), pp. 235 - 243. [10]